# Theoretical investigation of $\alpha$-like quasimolecules in heavy nuclei

D. S. Delion,[1,2,3] A. Dumitrescu,[1,2] and V. V. Baran[1,4]

[1]*Horia Hulubei National Institute for R&D in Physics and Nuclear Engineering, 30 Reactorului, P.O. Box MG-6, RO-077125 Bucharest-Măgurele, România*

[2]*Academy of Romanian Scientists, 54 Splaiul Independenţei, RO-050085 Bucharest, România*

[3]*Bioterra University, 81 Gârlei, RO-013724 Bucharest, România*

[4]*Department of Physics, University of Bucharest, 405 Atomiştilor, POB MG-11, RO-077125 Bucharest-Măgurele, România*

(Received 27 March 2018; revised manuscript received 10 May 2018; published 6 June 2018)

Quasimolecular $\alpha$-like ground rotational bands were evidenced a long time ago in light nuclei, but they cannot be detected in heavy nuclei due to large Coulomb barriers. In order to search for rotational bands built on excited states in these nuclei, we investigate the shape of an $\alpha$-nucleus quasimolecular potential matched to a realistic external $\alpha$-daughter interaction by using as input data $\alpha$-decay widths. It turns out that its Gaussian length parameter lies in a narrow interval, $b_0 \in [0.6,0.8]$ fm, and the equilibrium radius is slightly larger than the predicted Mott transition point from nucleonic to the $\alpha$-cluster phase in finite nuclei, confirming that $\alpha$ clusters are born on the nuclear surface at low densities. We point out that the $\alpha$ emitters above magic nuclei have the largest spectroscopic factors $S_\alpha \sim 10\%$. In addition, we predict that for nuclei with $b_0 > 0.75$ fm, the first excited vibrational resonant state in the quasimolecular potential is close to the Coulomb barrier and therefore the rotational band built on it can be evidenced by the structure of the $\alpha$-scattering cross section versus energy. Moreover, its detection by a highly sensitive $\gamma$-ray beam produced by laser facilities would provide an additional proof for the existence of $\alpha$ molecules in heavy nuclei.

DOI: 10.1103/PhysRevC.97.064303

## I. INTRODUCTION

The $\alpha$-decay between ground states is energetically not allowed in light nuclei, but many transitions from excited states were measured. As a characteristic feature, $\alpha$-like states with large spectroscopic factors were detected in this region [1,2]. The existence of $\alpha$-daughter quasimolecular rotational bands in such nuclei is a well established fact [3]. As a rule, they are connected to the anomalous large angle scattering (ALAS), where the differential cross sections of $\alpha$ particles are large compared to the Rutherford values for such nuclei [4]. The spontaneous emission of $\alpha$ particles from nuclei with $Z \geqslant 50$ has been interpreted as the penetration of "preformed" clusters through the Coulomb barrier near the region of the nuclear interaction [5,6]. The decay width can be expressed within the $R$-matrix theory as a product between the $\alpha$-cluster reduced width and the penetrability through the barrier [7]. The importance of $\alpha$ clustering in the nuclear structure above double magic nuclei was stressed not only for light, but also for heavy systems [8–10]. It is a well established fact that the absolute value of the $\alpha$-decay width cannot be described without an important clustering component mixed with standard shell orbitals [11]. A useful tool to investigate the $\alpha$ clustering in heavy and superheavy nuclei is given by the $\alpha$ decay to excited states. An important result concerning the quasimolecular interpretation of final $\alpha$-daughter rotating configurations is given in Ref. [12]. There, it was shown that the strength of the $\alpha$-daughter quadrupole-quadrupole interaction reproducing the experimental decay widths to $2^+$ states in even-even nuclei has significantly larger values above magic nuclei and rapidly decreases by adding $\alpha$-cluster configurations. For these nuclei, the spectroscopic factor has also larger values and therefore the rotating $\alpha$-daughter molecular $[L^+ \otimes L^+]_0$ configurations have relatively large probabilities. These configurations should exist at small densities beyond the nuclear surface, due to the fact that the Pauli principle prohibits the existence of $\alpha$ clusters inside nuclei [13,14].

The purpose of this paper is to show that it is possible to determine an $\alpha$-nucleus quasimolecular potential by using decay widths and a realistic $\alpha$-daughter interaction given by independent scattering data. The parameters of this potential allow one to predict the position of excited resonant states, which can in principle be detected in the excitation response function and therefore confirm the existence of $\alpha$ molecules in heavy nuclei. The paper is organized as follows: in Sec. II we prescribe the parameters of the internal pocketlike potential by using partial $\alpha$-decay data, in Sec. III we give a systematics of these parameters, and in the last section we draw conclusions.

## II. THEORETICAL BACKGROUND

The dynamics of two composite objects, like the $\alpha$-daughter system, is described within the resonating group method (RGM). The Pauli exchange effects lead to the occurrence of a repulsive core in the Hamiltonian kernel [15,16]. Thus, an effective energy dependent pocketlike local potential simulating the Pauli principle for $\alpha$ decay can be introduced [17]. For the emission process from a parent ($P$) state with angular momentum/parity $I_P$ to different daughter

 

$(D)-\alpha$-particle configurations $[I\otimes L]_{I_P}$,

$$P(I_P)\rightarrow D(I)+\alpha(L), \tag{2.1}$$

the wave function describing the $\alpha$-daughter motion can be expanded as follows:

$$\Psi^{(P)}_{I_PM_P}(\mathbf{R})=\sum_{c=1}^{N}\frac{\psi_c(R)}{R}\mathcal{Y}_c(\Omega,\hat{R}), \tag{2.2}$$

where $c=(I,L,I_P)$ is the channel index of the process, including parity values. The core-angular harmonics, depending on the daughter coordinates $\Omega$ and $\alpha$-particle angles $\hat{R}$, are defined by [18]

$$\mathcal{Y}_c(\Omega,\hat{R})=[\Psi^{(D)}_I(\Omega)\otimes Y_L(\hat{R})]_{I_PM_P}. \tag{2.3}$$

This wave function is a resonant outgoing solution of the stationary Schrödinger equation, called a Gamow state. For $\alpha$ decays from the ground states (gs) of even-even nuclei with $I_p=0^+$, one has $c=I=L=$ even,

$$\mathcal{Y}_L(\Omega,\hat{R})=\left[\Psi^{(D)}_L(\Omega)\otimes Y_L(\hat{R})\right]_0. \tag{2.4}$$

In the case of deformed rotational nuclei, one has $\Psi^{(D)}_{LM}(\Omega)=Y_{LM}(\Omega)$, and the final state corresponds to a "quasimolecular" rotational picture in which the daughter nucleus and $\alpha$ particle rotate in opposite directions with total momentum $I_P=0$. For vibrational nuclei, $\Psi_{LM}$ is a vibrational wave function and the picture corresponds to a "quasimolecule" where the two partners vibrate in opposite directions.

For transitions from odd-mass nuclei, $I_P$ and $I$ have half-integer values and the $\alpha$ particles are emitted with angular momenta $|I_P-I|\leqslant L\leqslant I_P+I$. The resonant states have positive parity for $L=$ even and negative parity for $L=$ odd. The daughter wave function has a core-quasiparticle ansatz

$$\Psi^{(D)}_{IM}(\Omega,\mathbf{r})=\sum_{Jj}X^I_{Jj}[\Phi_J(\Omega)\otimes\phi_j(\mathbf{r})]_{IM}, \tag{2.5}$$

where the coefficients are found by diagonalizing a core-quasiparticle interaction reproducing the energy spectrum. Notice that a rotational band with $I\geqslant j$ is defined by considering only a given quasiparticle orbital $j$ in the above superposition.

Let us mention that the coherent state model (CSM) treatment describes the two limits in a unified way by changing a "deformation parameter" $d$, which enters the coherent superposition of quadrupole bosons $\exp(db^\dagger_{2K})$ [12].

The $\alpha$-daughter dynamics is described by the stationary Schrödinger equation

$$H\Psi_{I_PM_P}(\Omega,\mathbf{R})=Q_\alpha\Psi_{I_PM_P}(\Omega,\mathbf{R}), \tag{2.6}$$

where $Q_\alpha$ is the relative energy of the emitted $\alpha$ particle, called the $Q$ value of the decay process. The stationarity is a very good assumption due to the fact that all measured decay widths are by many orders of magnitude smaller than the corresponding $Q$ values. Hence, an $\alpha$-decaying state is identified with a narrow resonant solution that contains only outgoing components. The Hamiltonian

$$H=-\frac{\hbar^2}{2\mu}\nabla^2_R+H_D(\Omega)+V_0(\Omega,R)+V_d(\Omega,\mathbf{R}) \tag{2.7}$$

contains the kinetic operator, depending on the reduced mass $\mu=m_N4A_D/(4+A_D)$, a term describing the dynamics of the nuclear core $H_D(\Omega)$,

$$H_D\Psi^{(D)}_{IM_I}(\Omega)=E_c\Psi^{(D)}_{IM_I}(\Omega), \tag{2.8}$$

and the $\alpha$-core interaction, which we split into spherical and deformed parts. By using the orthonormality of the core-angular harmonics in the superposition (2.2), one obtains in a standard way the system of differential equations for radial components [18],

$$\frac{d^2\psi_c(R)}{d\rho_c^2}=\sum_{c'=1}^{N}A_{cc'}(R)\psi_{c'}(R), c=1,\ldots,N, \tag{2.9}$$

where the coupling matrix is given by

$$A_{cc'}(R)=\left[\frac{L_c(L_c+1)}{\rho_c^2}+\frac{V_0(\Omega,R)}{Q_\alpha-E_c}-1\right]\delta_{cc'}+\frac{\langle\mathcal{Y}^{(c)}_{I_p}|V_d(\Omega,\mathbf{R})|\mathcal{Y}^{(c')}_{I_p}\rangle}{Q_\alpha-E_c}, \tag{2.10}$$

in terms of the channel reduced radius,

$$\rho_c=\kappa_cR,\quad \kappa_c=\sqrt{\frac{2\mu(Q_\alpha-E_c)}{\hbar^2}}. \tag{2.11}$$

Let us mention that at large distances the potential becomes spherical ($V_d\rightarrow 0$) and purely Coulombian. The external solutions in each channel $c$ can be found by superposition,

$$\psi^{(\mathrm{ext})}_c(R)=\sum_{a=1}^{N}\mathcal{H}^{(+)}_{ca}(R)\mathcal{N}_a. \tag{2.12}$$

Here we have involved the columns of the fundamental matrix of Coulomb solutions with outgoing Coulomb-Hankel asymptotics,

$$\mathcal{H}^{(+)}_{ca}(R)=\mathcal{G}_{ca}(R)+i\mathcal{F}_{ca}(R)\longrightarrow[R\rightarrow\infty]\,\delta_{ca}H^{(+)}_{L_c}(R)=\delta_{ca}\left[G_{L_c}(R)+iF_{L_c}(R)\right], \tag{2.13}$$

where $c$ denotes the channel and $a$ is the resonant eigenvalue index. Inside the Coulomb barrier, its modulus practically coincides with the real matrix of irregular Coulomb solutions $|\mathcal{H}^{(+)}_{ca}(R)|\approx\mathcal{G}_{ca}(R)$. The unknown coefficients $\mathcal{N}_a$ are called scattering amplitudes.

From the continuity equation one obtains the total decay width as a sum of partial widths [18],

$$\Gamma=\sum_c\Gamma_c=\sum_c\hbar v_c\lim_{R\rightarrow\infty}|f_c(R)|^2=\sum_c\hbar v_c|\mathcal{N}_c|^2, \tag{2.14}$$

depending on scattering amplitudes and asymptotic velocities $v_c=\kappa_c/\mu$. By inverting Eq. (2.12) and using (2.14), the external components of the wave function at some point $R$ inside the $\alpha$-daughter potential can be expressed as

$$\psi^{(\mathrm{ext})}_c(R)=\sum_{a=1}^{N}\mathcal{H}^{(+)}_{ca}(R)\sqrt{\frac{\Gamma_a}{\hbar v_a}},\quad c=1,\ldots,N, \tag{2.15}$$

in terms of the partial decay widths $\Gamma_a$ and asymptotic channel velocities.

Let us mention that for the spherical one-channel limit with $L_c = 0$, by considering the matching condition $\psi^{(\mathrm{int})}(R) = \psi^{(\mathrm{ext})}(R)$, Eq. (2.15) becomes the well known relation

$$\Gamma_0 = \hbar v_0 \left[ \frac{\psi_0^{(\mathrm{int})}(R)}{\mathcal{G}_{00}(R)} \right]^2. \tag{2.16}$$

Microscopic calculations within the mean field plus pairing approach evidenced that the $\alpha$-formation amplitude has a shifted Gaussian shape with a maximum located beyond the nuclear surface [18] and is mainly concentrated in the monopole component. Moreover, this conclusion is supported by a systematic phenomenologic analysis of all particle/cluster emission processes [19]. Our coupled channel analysis confirmed such a behavior for the internal part of resonant solutions [12],

$$\psi_0^{(\mathrm{int})}(X) = A_0 \sqrt{\frac{1}{N}} \sqrt{\frac{\beta_0}{\pi}} e^{-\beta_0 X^2/2}, \tag{2.17}$$

where $X = R - R_0$ is the shifted radial coordinate and $N$ is the number of channels. Here, $A_0$ denotes the cluster amplitude and $\beta_0$ is the harmonic oscillator (ho) parameter of the monopole component,

$$\beta_0 = \frac{1}{b_0^2} = \frac{m_\alpha \omega_0}{\hbar} = f \hbar \omega_0,$$
$$f \equiv \frac{m_\alpha c^2}{(\hbar c)^2} \sim 0.096\ (\mathrm{MeV}^{-1}\,\mathrm{fm}^{-2}), \tag{2.18}$$

which can be written in terms of the ho length parameter $b_0$. Here we considered that for heavy nuclei one has $\mu \approx m_\alpha$. This wave function is generated by a shifted ho $\alpha$-daughter local potential,

$$V_0^{(\mathrm{int})}(X) = v_0 + \frac{1}{2} \hbar \omega_0 \beta_0 X^2. \tag{2.19}$$

We match this potential to a realistic external interaction. We considered in our analysis the double folding $\alpha$-nucleus potential computed by using an $M3Y$ nucleon-nucleon plus Coulomb proton-proton interaction [12]. The parameters are determined from $\alpha$-scattering experiments. For the $\alpha$ particle, we assumed a Gaussian distribution with $b_\alpha = 1.19$ fm [20,21].

Let us match the internal shifted ho potential to the monopole component of the external double folding potential $V_0(R)$ and do the same for the wave function. Doing so, we can determine the unknown coefficients $v_0$, $\beta_0$, and $R_0$, by means of the following matching relations:

$$v_0 + \frac{1}{2f} \beta_0^2 X_m^2 = V_0(R_m), \quad X_m = R_m - R_0,$$
$$\frac{1}{f} \beta_0^2 X_m = V_0'(R_m),$$
$$\ln' \psi_0^{(\mathrm{int})}(X_m) = -\beta_0 X_m = \ln' \psi_0^{(\mathrm{ext})}(R_m). \tag{2.20}$$

In the standard coupled channels procedure we fix the $Q$ value by using $v_0$, thus obtaining from the first two equations the equality

$$X_m = \frac{2[V_0(R_m) - v_0]}{V_0'(R_m)}, \tag{2.21}$$

which determines the ho parameter $\beta_0$.

In our analysis, the $Q$ value is given by experimental data and therefore one directly obtains the ho parameter and $X_m$ from the last two equations,

$$\beta_0 = -\frac{f V_0'(R_m)}{\ln' \psi_0^{(\mathrm{ext})}(R_m)}$$
$$= -\frac{\ln' \psi_0^{(\mathrm{ext})}(R_m)}{X_m} = \sqrt{\frac{f V_0'(R_m)}{X_m}}. \tag{2.22}$$

We fix the matching radius at the second internal turning point $R_m = R_{\mathrm{int}}$. This choice ensures the existence of a narrow resonance corresponding to the first eigenvalue in the ho pocket with $Q - v_0 \sim \frac{1}{2}\hbar\omega_0$. Thus, one determines $\beta_0$ and $X_m$, and therefore the equilibrium radius $R_0$. The value of $v_0$ is given by the first equation (2.20).

Due to the centrifugal barrier in each channel with angular momentum $L$, the channel wave functions will be given by Gaussians with slightly different ho parameters

$$\psi_c^{(\mathrm{int})}(X) = A_c \sqrt{\frac{1}{N}} \sqrt{\frac{\beta_c}{\pi}} e^{-\beta_c X^2/2}. \tag{2.23}$$

The ho parameters and amplitudes will be determined by the standard matching conditions

$$\beta_c = -\frac{1}{X_M} \ln' \psi_c^{(\mathrm{ext})}(R_m),$$
$$A_c = \psi_c^{(\mathrm{ext})}(R_m) \sqrt{N \sqrt{\frac{\pi}{\beta_c}}} e^{\beta_c X_m^2/2}. \tag{2.24}$$

External components have much smaller values than internal components in the internal region $R \in [0, R_m]$. Therefore the $\alpha$-particle spectroscopic factor is given by

$$S_\alpha = \int |\Psi(\mathbf{R})|^2 d\mathbf{R} \sim \sum_c A_c^2 \equiv \sum_c S_c. \tag{2.25}$$

## III. NUMERICAL APPLICATION

We first analyzed the above defined resonant eigenstates in the pocketlike $\alpha$-core potential. In Fig. 1 we plotted a typical spectrum of resonant states for the transition $^{144}\mathrm{Nd} \rightarrow {}^{140}\mathrm{Ce} + \alpha$. This system was under scrutiny in Ref. [22].

The first resonant zero node state has the eigenvalue $E_0$ corresponding to the $Q$ value of the process, drawn by the lower solid line. Obviously, the experimental decay width between ground states is reproduced.

Lower solid and dotted lines are eigenstates in the parent nucleus with $J_P = 0^+$, described by coupling the low-lying eigenstates of the daughter nucleus with $\alpha$-particle states $[L \otimes L]_0$ in Eq. (2.4). Each eigenstate has one $L$-dominant component with a probability depending on deformation. Its energy contains the daughter energy $E_c$ plus centrifugal $\alpha$-particle energy plus a coupling correction term. We considered

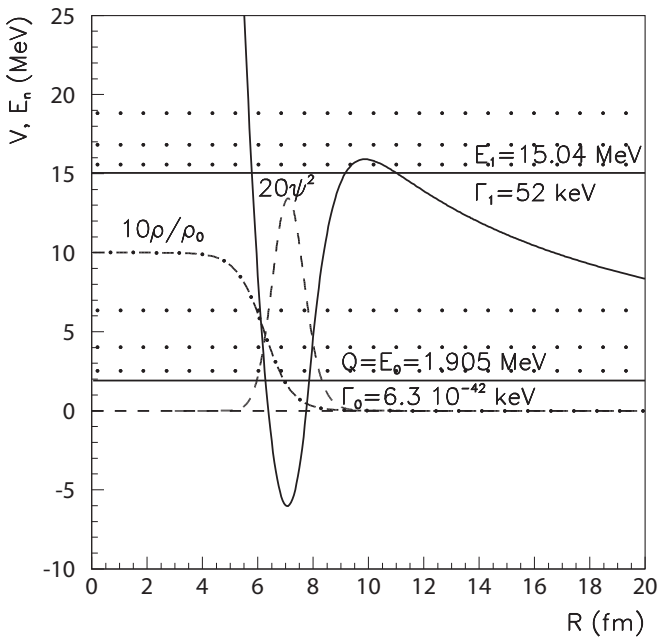


FIG. 1. Vibrational resonant states (solid lines) and rotational bands built on them (dotted lines) in the $\alpha$-$^{140}$Ce molecular potential. The lower solid line corresponds to the $Q$ value of the process. The dot-dashed line is ten times the ratio $\rho(R)/\rho_0$ and the dashed line shows a factor 20 multiplying the gs $\alpha$-particle probability vs radius.

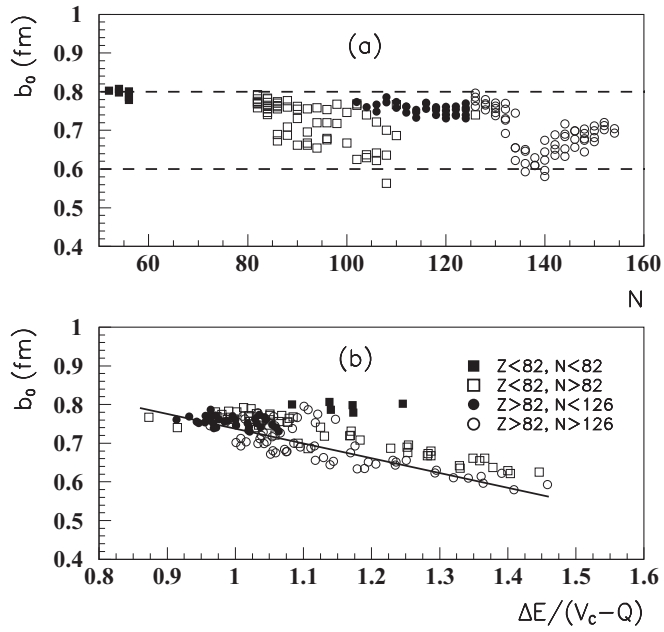


FIG. 2. Monopole ho length parameter vs neutron number of the daughter nucleus (a) and vs the ratio between the energy difference of vibrational levels and fragmentation potential (b) for even-even emitters. The symbols denote different regions of the nuclear chart, divided by magic numbers. The regression line in panel (b) fits the data, excepting the first region (dark squares).

experimental energies of the daughter nucleus in the coupled system of equations (2.9) and (2.10). A systematic analysis of their $B(E2)$ values is given in Ref. [12]. In Ref. [10], we have shown that for $^{212}$Po the low-lying $0^+\alpha$-like resonances (except gs) have small spectroscopic factors and they can be experimentally detected only above 6 MeV. We expect similar properties for low lying monopole resonances plotted by dotted lines in Fig. 1. Therefore, they cannot be detected experimentally and the $0^+$ states observed around 2 MeV in $^{144}$Nd have a different nature. The upper solid line denotes the eigenvalue $E_1$ of the first one-node excited vibrational state and the dotted lines above it belong to the excited monopole band with $J_P = 0^+$. The decay width $\Gamma_0$ in Fig. 1 is given by the barrier penetration $\Gamma_{\rm pen} = 5 \times 10^{-41}$ keV multiplied with the spectroscopic factor $S_\alpha = 0.125$ and it reproduces the input experimental value $\Gamma_{\rm exp} = 6.3 \times 10^{-42}$ keV. Moreover, our numerical estimate gives a ratio between errors $\delta\Gamma_1/\delta E_1 = 0.16$.

Obviously, the energy difference $\Delta E = E_1 - E_0$ determines the ho parameter of the molecular potential. We plotted the wave function multiplied by a factor of 20 with a dashed line, and with a dot-dashed line the ratio between the nuclear and equilibrium density multiplied by 10,

$$\frac{\rho(R)}{\rho_0} = \frac{1}{1+\exp[(R-R_n)/a]}, \tag{3.1}$$

by considering a standard diffusivity parameter $a = 0.5$ fm and nuclear radius $R_n = 1.2A^{1/3}$. These standard values are close to the systematics of Ref. [23] based on electron scattering data. Let us mention that the Mott phase transition point between the nucleonic and $\alpha$-clustering phases corresponds to about 10% of the equilibrium density in infinite nuclear matter [13] and 20% for $^{212}$Po, as seen in Fig. 5 of Ref. [14]. Thus, our calculation confirms that the maximal value of the wave function corresponds to a radius larger than the phase transition point.

As we mentioned, the rotational quasimolecular band is connected to the ALAS phenomenon. In Ref. [24] was pointed out that the experimental evidence of this effect was found for a lighter configuration with $Z = 40$, namely $\alpha + ^{90}$Zr. Anyway, one sees from Refs. [25,26] that for the configuration analyzed above, $\alpha + Ce$ with $Z = 58$, the ALAS phenomenon disappears close to the Coulomb barrier $V_C \sim 16$ MeV, due to the fact that exchange effects diminish for $Z > 50$.

In Fig. 2(a), we plotted the ho length parameter $b_0$ of the gs channel with $L = 0$ versus the neutron number of the daughter nucleus for 162 even-even emitters. Notice that $b_0 \in [0.6,0.8]$ fm, i.e., the ratio to the standard $\alpha$-particle length parameter $b_\alpha = 1.19$ fm belongs to a rather narrow interval $b_0/b_\alpha \in [0.5,0.7]$. In the lower panel (b), we plotted the length parameter versus the ratio between the energy difference of vibrational levels $\Delta E = E_1 - E_0$ and the fragmentation potential $V_{\rm frag} = V_C(R_{\rm max}) - Q$. Notice that $V_{\rm frag} \in [10,17]$ MeV. Except for the first region, $Z \sim N \sim 50$ of "superallowed" $\alpha$ transitions [27], these quantities are linearly correlated. For nuclei with $b_0 > 0.75$ fm, the rotational band built on the first excited state lies close to the Coulomb barrier $\Delta E/V_{\rm frag} \sim 1$ and therefore it can be seen as a structure of maxima in the energy dependent cross section. The linear correlation between the length ho parameter $b_0$ and the ratio $\Delta E/V_{\rm frag}$ gives predictive power to this parametrization of

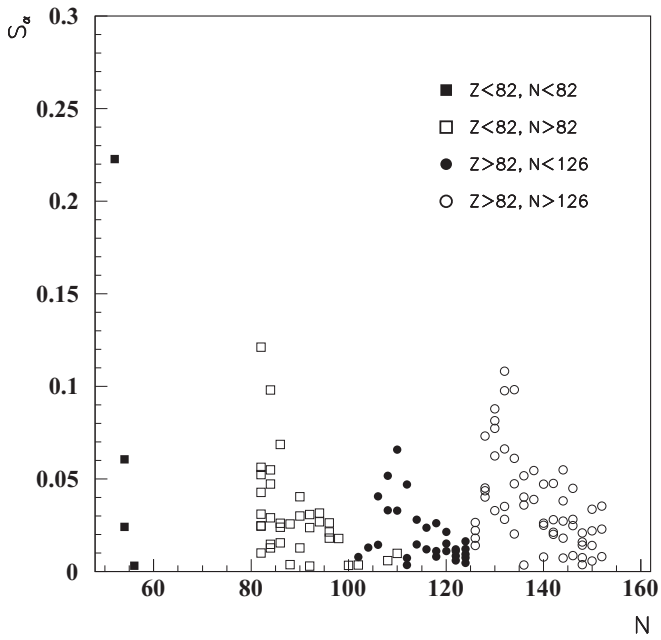


FIG. 3. Spectroscopic factor vs neutron number of the daughter nucleus for even-even emitters. The symbols denote different regions of the nuclear chart divided by magic numbers.

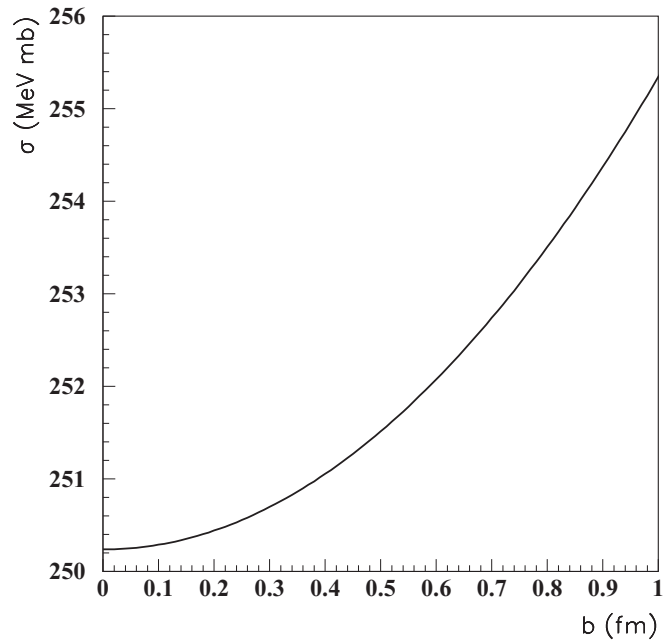


FIG. 4. Absorbtion energy-integrated cross section vs the ho length parameter given by Eq. (3.2) for $r_0 = 7$ fm.

the internal pocketlike potential, because the fragmentation potential is experimentally determined and $\Delta E$ is directly related to $b_0$. The regression line in Fig. 2(b), fitting the data excepting the first region (dark squares), gives a mean error $\langle \delta b_0 \rangle = 0.03$ fm.

In Fig. 3, we plotted the spectroscopic factor (2.25) versus the neutron number of the daughter nucleus. We notice large values above the magic numbers $Z = 50,82$ and $N = 82,126$, where $\alpha$ molecules are born with significant probabilities [12] and the best candidates for experimental detection have $\Delta E / V_{\rm frag} \sim 1$.

The fine structure of odd-mass emitters was measured for $Z \in [87,100]$. Here, one obtains $b_0/b_\alpha \in [0.6,0.7]$ and $\Delta E / V_{\rm frag} \in [0.8,1.0]$. Additionally, the $L = 1$ angular momentum of the emitted $\alpha$ particle is allowed. Thus, the lower and upper vibrational eigenstates in the pocketlike potential of Fig. 1 can be connected by a dipole operator $D \sim X = R - R_0$ of the $\alpha$-particle center of mass. Therefore, the second vibrational state can be detected in the excitation function of an incident $\gamma$ beam. Such beams are produced at operating $\gamma$-beam facilities, and will be provided in the future at the ELI-NP facility [28].

The total absorbtion energy-integrated cross section for the transition between the first $n = L = 0$ and second vibrational levels $n = L = 1$ in the shifted ho potential can be estimated in a standard way as a function of the ho length parameter,

$$\sigma = \sigma_0 \left[ 1 + \left( \frac{b_0}{R_n} \right)^2 \right],$$
$$\sigma_0 = \frac{8\pi^3}{3} \frac{\hbar c}{m_\alpha c^2} e_\alpha^2 \sim 250 \text{ MeV mb}. \qquad (3.2)$$

In Fig. 4 we plotted the dependence of the energy-integrated cross section versus the ho length parameter. It has significant values, $\sigma \sim \sigma_0 \sim 250$ MeV mb, which can be detected experimentally. Let us mention that this kind of $\alpha$-like resonance was recently analyzed in Ref. [29] within a semiclassical approach. There, the coupling with GDR and pygmy modes was considered, and the EWSR was estimated. It was concluded that the alpha mode exceeds the pygmy EWSR fraction even for a relatively large neutron excess. The experimental signature of the $\alpha$-like state is a larger $\alpha$-decay width.

## IV. CONCLUSIONS

We have shown that it is possible to determine the shape of the $\alpha$ clusters on the nuclear surface by using as input data partial decay widths. We matched the logarithmic derivatives of the external wave function components to internal Gaussian wave functions corresponding to a shifted ho $\alpha$-nucleus interaction and determined the ho parameter and equilibrium radius. The equilibrium radius is slightly larger than the Mott transition point from nucleonic to the $\alpha$-cluster phase in finite nuclei. We predict that the first excited vibrational resonant state in the quasimolecular $\alpha$-daughter potential is close to the Coulomb barrier for nuclei with $b_0 > 0.75$ fm and therefore its rotational band can in principle be evidenced as a structure of maxima in the $\alpha$-particle scattering cross section. The associated ALAS phenomenon diminishes due to the hindrance of the $\alpha$-exchange effects. Moreover, the dipole excitation of the $n = L = 1$ state by $\gamma$ rays in odd-mass emitters would provide an additional proof for the existence of $\alpha$ molecules in heavy nuclei.

**ACKNOWLEDGMENTS**

This work was supported by the grants of the Romanian Ministry of Research and Innovation, CNCS - UEFISCDI, PN-III-P4-ID-PCE-2016-0092, PN-III-P4-ID-PCE-2016-0792, within PNCDI III, and PN-18090101/2018. We are grateful to Prof. N. V. Zamfir (ELI-NP) for his remarks.

[1] P. Schuck, Y. Funaki, H. Horiuchi, G. Röpke, A. Tohsaki, and T. Yamada, Phys. Scr. **91**, 123001 (2016).
[2] A. Tohsaki, H. Horiuchi, P. Schuck, and G. Röpke, Rev. Mod. Phys. **89**, 011002 (2017).
[3] W. von Oertzen, M. Freer, and Yoshiko Kanada-Enyo, Phys. Rep. **432**, 43 (2006).
[4] H. Abele and G. Staudt, Phys. Rev. C **47**, 742 (1993).
[5] G. Gamow, Z. Phys. **51**, 204 (1928).
[6] E. U. Condon and R. W. Gurney, Nature (London) **122**, 439 (1928).
[7] A. M. Lane and R. G. Thomas, Rev. Mod. Phys. **30**, 257 (1958).
[8] Y. K. Gambhir, P. Ring, and P. Schuck, Phys. Rev. Lett. **51**, 1235 (1983).
[9] B. Buck, A. C. Merchant, and S. M. Perez, Phys. Rev. C **51**, 559 (1995).
[10] D. S. Delion and J. Suhonen, Phys. Rev. C **61**, 024304 (2000).
[11] K. Varga, R. G. Lovas, and R. J. Liotta, Phys. Rev. Lett. **69**, 37 (1992); Nucl. Phys. A **550**, 421 (1992).
[12] D. S. Delion and A. Dumitrescu, At. Data Nucl. Data Tables **101**, 1 (2015).
[13] G. Röpke, A. Schnell, P. Schuck, and P. Nozieres, Phys. Rev. Lett. **80**, 3177 (1998).
[14] G. Röpke, P. Schuck, Y. Funaki, H. Horiuchi, Z. Ren, A. Tohsaki, C. Xu, T. Yamada, and B. Zhou, Phys. Rev. C **90**, 034304 (2014).
[15] L. F. Canto and D. M. Brink, Nucl. Phys. A **279**, 85 (1977).
[16] T. Fliessbach and H. Walliser, Nucl. Phys. A **377**, 84 (1982).
[17] R. G. Lovas, R. J. Liotta, A. Insolia, K. Varga, and D. S. Delion, Phys. Rep. **294**, 265 (1998).
[18] D. S. Delion, *Theory of Particle and Cluster Emission* (Springer-Verlag, Berlin, 2010).
[19] D. S. Delion, Phys. Rev. C **80**, 024310 (2009).
[20] G. Bertsch, J. Borysowicz, H. McManus, and W. G. Love, Nucl. Phys. A **284**, 399 (1977).
[21] G. R. Satchler and W. G. Love, Phys. Rep. **55**, 183 (1979).
[22] P. Mohr, Phys. Rev. C **61**, 045802 (2000).
[23] H. de Vries, C. W. de Jager, and C. de Vries, At. Data Nucl. Data Tables **36**, 495 (1987).
[24] S. Ohkubo, Phys. Rev. Lett. **74**, 2176 (1995).
[25] B. D. Watson, D. Robson, D. D. Tolbert, and R. H. Davis, Phys. Rev. C **4**, 2240 (1971).
[26] P. Mohr, Phys. Rev. C **87**, 035802 (2013).
[27] V. V. Baran and D. S. Delion, Phys. Rev. C **94**, 034319 (2016).
[28] N. V. Zamfir, Eur. Phys. J.: Spec. Top. **223**, 1221 (2014); EPJ Web Conf. **66**, 11043 (2014).
[29] V. V. Baran and D. S. Delion, J. Phys. G **45**, 035106 (2018).